Author response to reviewer comments

Anonymous Referee #1

I appreciate the effort and work put into this manuscript, which focuses on constructing a dataset of SAR images annotated for 12 types of oceanic and atmospheric phenomena and developing a deep learning model to segment these phenomena. The paper addresses a significant topic and provides valuable contributions. However, several areas need to be addressed to improve the overall quality and clarity of the manuscript.

Thank you for your valuable comments and suggestions on our manuscript. Your detailed feedback has been instrumental in helping us improve the quality of our work. Below, we provide a detailed response to each of your specific comments and the corresponding revisions we have made.

Review comments in blue

Reply in black

1 Dataset：

Q1. The criteria for determining the boundaries of each phenomenon are not clearly defined. For example, the internal wave is identified by its wave crest lines, while the pure ocean wave includes both wave crest lines and surrounding seawater. The boundary size for eddies is not clearly defined, and typically, eddies detected by SAR are accompanied by biological slicks, which are not considered in the dataset.

This study focuses on 12 typical oceanic and atmospheric phenomena. For the 10 oceanic and atmospheric phenomena with existing research, we referenced the segmentation standards of Benchaabane et al., Wang et al. and Colin et al. (Benchaabane et al., 2022; Colin et al., 2022; Wang et al., 2019a). For the two newly added oceanic phenomena, oceanic eddies and oceanic internal waves, we established segmentation standards based on relevant literature, as follows:

1) For oceanic eddies: Oceanic eddies change sea surface roughness by carrying tracers (such as

sea ice and biological slicks) or affecting surface flow fields, creating distinct elliptical patches or bands on SAR images. Depending on their formation mechanisms, they are primarily categorized as "dark eddies" and "white eddies"(Ji et al., 2021; Kozlov et al., 2019; Stuhlmacher and Gade, 2020). In this manuscript, the minimum enclosing shape of the eddies is used as the ground truth label. Notably, biological slicks often serve as tracers for oceanic eddies, and in overlapping cases, the priority of identifying the eddy phenomenon is higher than that of the biological slick phenomenon.

2) For oceanic internal wave phenomenon: Oceanic internal waves appear in SAR images as irregular stripes of alternating light and dark patterns. To ensure accurate labeling, we referred to publicly available object detection datasets. (Tao et al., 2022a)for the annotation.

Q2. The sea ice regions in the images seem to include ice leads, yet the entire area is labeled as sea ice. Additionally, the separation between low wind speed areas and biological slicks or oil spills is not clearly explained.

Regarding the sea ice you mentioned, the marking of sea ice in the manuscript follows a similar logic to that of Wang et al.(Wang et al., 2019b), the goal is to distinguish sea ice from open water in the SAR images. Thus, the segmentation label creation focuses on delineating areas and does not achieve the precision required to segment out sea leads. We will continue to improve and refine the sea ice labeling.

For distinguishing low wind speed areas, biological slicks, and oil spills: Low wind speed areas often coexist with biological slicks. Low wind speed regions are characterized by large dark patches on the sea surface, while biological slicks appear as aggregated black filaments (Najoui et al., 2018). Oil spills typically manifest as isolated black filaments, and relevant oil spill datasets will be provided later.

Q3. Internal waves and eddies, particularly eddies, typically occur offshore. Using IW mode data limits the representation of these phenomena.

For oceanic eddy phenomena, to ensure data diversity, we selected images from both the Sentinel-1 IW mode and the WV mode from the TenGeoP-SARwv dataset, with a roughly equal number of images from each mode. (Although the TenGeoP-SARwv dataset does not include a category for oceanic Eddy, its classification of biological slicks contains a substantial number of oceanic Eddy phenomena.)

Regarding the oceanic internal wave images in the WV mode, their size limits the assessment of these waves (Colin et al., 2022). To ensure the accuracy of the evaluation, we use the Sentinel-1 IW mode ocean internal wave object detection dataset proposed by Tao et al. (Tao et al., 2022b) for data labeling.

Q4. Additionally, the manuscript mentions using 484 IW images to select samples of internal waves and eddies, but it is unclear where these images are located, how representative they are, and the criteria for their selection.

The IW mode images are divided into two parts. One part comes from the ocean internal wave dataset, while the other part consists of images from Sentinel-1 IW mode, selected from ASF (https://search.asf.alaska.edu/), featuring typical oceanic and atmospheric phenomena.

For the oceanic internal wave phenomenon, we selected images consistent with the dataset, which includes Andaman Sea, South China Sea, Sulu Sea, and Celebes Sea area (Tao et al., 2022b). We randomly selected 50 IW mode images from each study area for annotation.

For other phenomena, we selected Sentinel-1 IW mode images from 2021-2022 that exhibit typical characteristics of oceanic and atmospheric phenomena for annotation. We have added a distribution map of these SAR images in the revised manuscript.

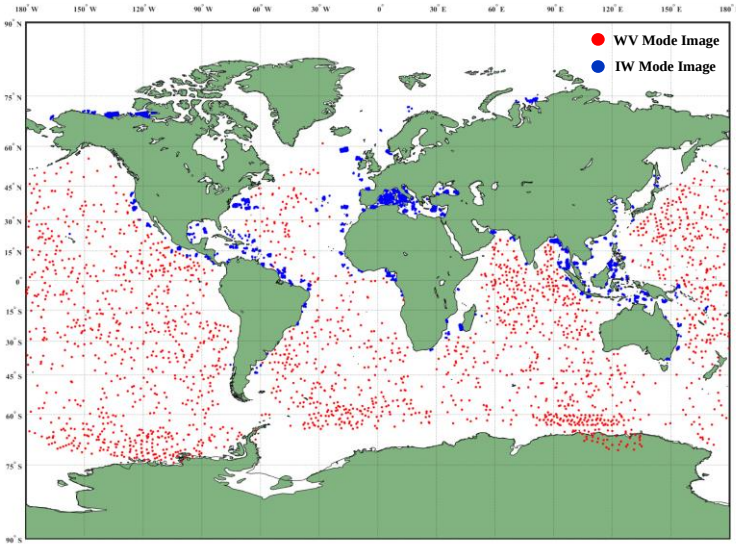

Phenomenon	Total
AF	644
BS	1034
IB	398
LWA	601
MCC	830
OF	437
POW	1746
RF	484
SI	454
WS	585
Eddy	501
IWs	417

Figure: The data distribution (red is WV mode, blue is IW mode) and the number of images for each category.

Q5. The TenGeoP-SARwv dataset (Wang et al., 2019), on which this study builds, does not provide geographical information, making it difficult for readers or users to assess the representativeness of the images.

In this study, we randomly selected images from the TenGeoP-SARwv dataset according to different

oceanic and atmospheric phenomena when constructing the dataset. We have updated the dataset to ensure it includes geographical information.

Q6. Except for the final rainfall image, the manuscript does not provide geographical coordinates for all the SAR images.

We have modified the SAR images in the manuscript to ensure that each image fully displays the latitude and longitude coordinate information.

2 Metric Calculation：

Q1. Many of the selected phenomena, such as fronts, internal waves, and icebergs, are significantly smaller in pixel count compared to the background (seawater). The manuscript does not exclude the background when calculating metrics, leading to potentially inflated performance scores.

In this manuscript, we have already excluded the background category when calculating the metrics. Taking mDice as an example, we first calculate the Dice coefficient for each category, and then we average the results for the 12 phenomena of interest, thus obtaining the mDice for these 12 phenomena, excluding the background category.

Q2. However, in the case of internal wave extraction (Figures 12 and 13), several rain cells are visible but not identified by the model.

In this manuscript, we selected ocean internal waves and rainfall phenomena for visual validation. To avoid interference from other phenomena, Figures 12 and 13 show only the segmentation results for ocean internal waves. The complete images of the following results are provided. The figures demonstrate that the rainfall phenomenon was successfully detected and identified, but it interfered with the visual interpretation of the ocean internal waves. Therefore, we have retained only the ocean internal wave phenomenon for analysis.

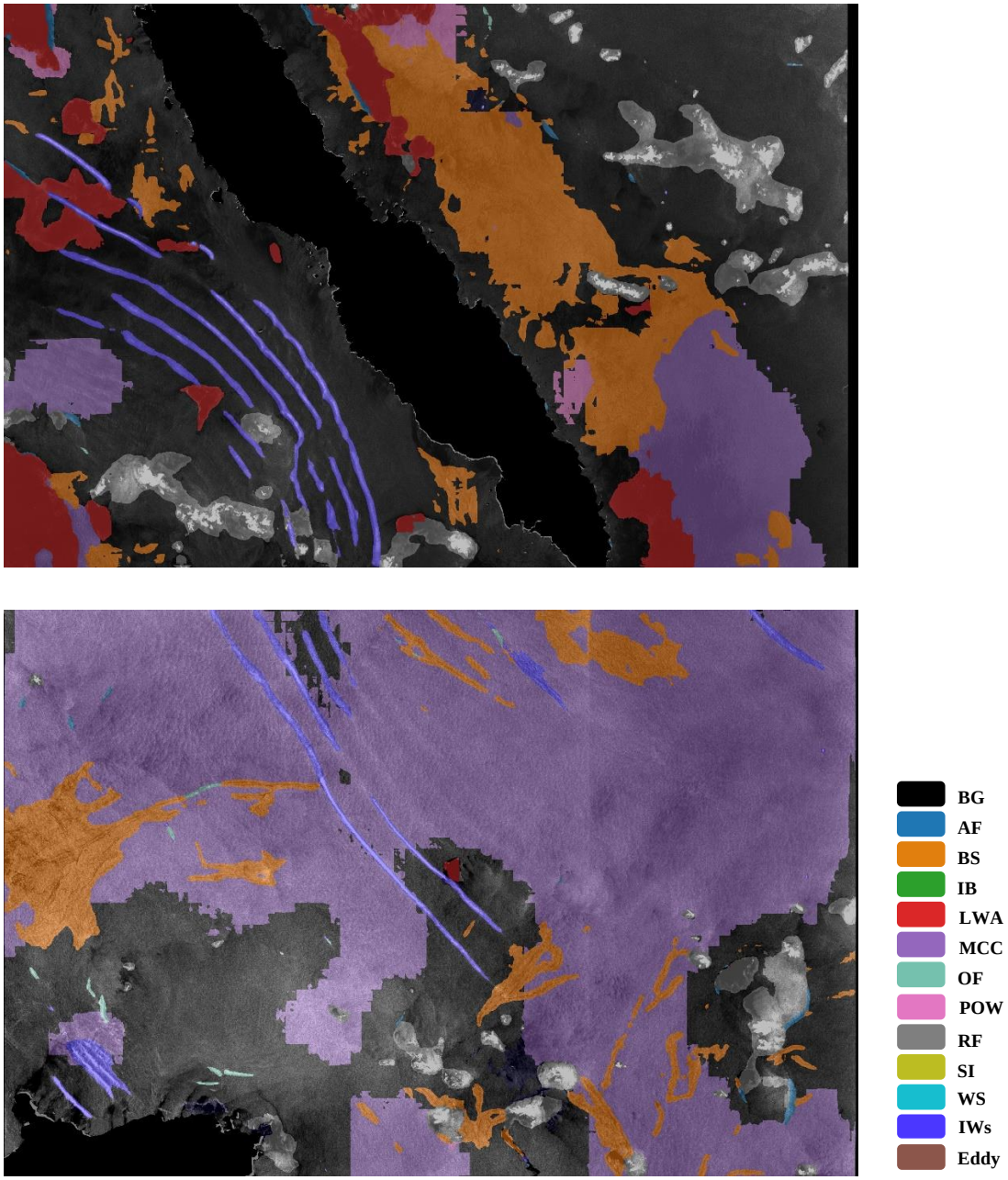

Figure: Complete test results (Figures 12 and 13). (The images are consistent with those in the first draft of the manuscript to facilitate comparison.)

Q3. The manuscript should include a comparison with ground truth and corresponding metrics for all phenomena.

In this manuscript, Figure 8 compares the segmentation results of five networks on the test set with the ground truth, while the corresponding metrics for all phenomena are presented in Table 2.

Q4. Additionally, the rationale for selecting only internal waves and rain cells for demonstration should be clarified (Section 4.4).

In SAR images, the overlap of different phenomena often occurs, which poses significant challenges

for semantic segmentation tasks. We selected oceanic internal waves and rainfall—two typical oceanic and atmospheric phenomena—for validation because they cause substantial changes in sea surface roughness, making overlap with other phenomena less likely. This ensures a clearer visual interpretation and more reliable assessment of the segmentation results. We have already stated this in the article.

Q5. The use of GPM half-hour rainfall data introduces temporal and spatial discrepancies with SAR imaging, which should be acknowledged. Figure 16 illustrates a noticeable discrepancy in the center location of the rainfall. It is recommended to define the criteria for identifying rain cells and directly compare them with ground truth rather than relying on GPM data.

We have restated in the article that there are certain discrepancies between the GPM rainfall data and SAR images. Regarding your mention of comparing dynamic annotations with segmentation results, we have performed similar comparison validation on the test set (Figure 8). The main objective of this section is to perform comparative validation with external data. Comparing manually labeled annotations with segmentation results may introduce a certain level of subjectivity, making it challenging to ensure the accuracy of the segmentation results.

3 Others

Q1. Geographical Coordinates and Imaging Time: Remote sensing images should include geographical coordinates and imaging time, which are crucial in geoscience research.

We have updated the SAR images in the manuscript to accurately display the geographic coordinates and the time of image capture.

Q2. Terminology and Labeling: On line 289, page, ‘individual’ might not be accurate. It is a group approaching the shore (Figure 13b).

We have revised the inaccurate statements accordingly. (L329)

Q3. The abbreviation IW is ambiguous and can refer to both Sentinel-1 imaging mode and internal waves.

We have made revisions to the manuscript. “IW” refers to the Sentinel-1 IW mode, while “IWs” stands for Internal Waves.

Q4. The term BG in the figures is not explained in the text.

"BG" refers to the background classification, which indicates the sea surface outside the phenomena of interest. We have included a definition of this in the manuscript.

Q5. Units and numbers should have a space in between (e.g., lines 348 and 349, page 14).

We have made the modifications in the manuscript. (L387)

Reference

Benchaabane, A., Peureux, C., and Soulat, F.: A labelled dataset description for SAR images segmentation, 2022.

Colin, A., Fablet, R., Tandeo, P., Husson, R., Peureux, C., Longépé, N., and Mouche, A.: Semantic Segmentation of Metoceanic Processes Using SAR Observations and Deep Learning, Remote Sensing, 14, 851, https://doi.org/10.3390/rs14040851, 2022.

Ji, Y., Xu, G., Dong, C., Yang, J., and Xia, C.: Submesoscale eddies in the East China Sea detected from SAR images, Acta Oceanol. Sin., 40, 18–26, https://doi.org/10.1007/s13131-021-1714-5, 2021.

Kozlov, I. E., Artamonova, A. V., Manucharyan, G. E., and Kubryakov, A. A.: Eddies in the Western Arctic Ocean From Spaceborne SAR Observations Over Open Ocean and Marginal Ice Zones, J. Geophys. Res. Oceans, 124, 6601–6616, https://doi.org/10.1029/2019JC015113, 2019.

Najoui, Z., Riazanoff, S., Deffontaines, B., and Xavier, J.-P.: A statistical approach to preprocess and enhance c-band SAR images in order to detect automatically marine oil slicks, IEEE Trans. Geosci. Remote Sens., 56, 2554–2564, 2018.

Stuhlmacher, A. and Gade, M.: Statistical analyses of eddies in the Western Mediterranean Sea based on Synthetic Aperture Radar imagery, Remote Sensing of Environment, 250, 112023, 2020.

Tao, M., Xu, C., Guo, L., Wang, X., and Xu, Y.: An Internal Waves Data Set From Sentinel-1 Synthetic Aperture Radar Imagery and Preliminary Detection, Earth Space Sci., 9, e2022EA002528, https://doi.org/10.1029/2022EA002528, 2022a.

Tao, M., Xu, C., Guo, L., Wang, X., and Xu, Y.: An Internal Waves Data Set From Sentinel-1 Synthetic Aperture Radar Imagery and Preliminary Detection, Earth Space Sci., 9, e2022EA002528, https://doi.org/10.1029/2022EA002528, 2022b.

Wang, C., Mouche, A., Tandeo, P., Stopa, J. E., Longépé, N., Erhard, G., Foster, R. C., Vandemark, D., and Chapron, B.: A labelled ocean SAR imagery dataset of ten geophysical phenomena from Sentinel-1 wave mode, Geosci. Data J., 6, 105–115, https://doi.org/10.1002/gdj3.73, 2019a.

Wang, C., Tandeo, P., Mouche, A., Stopa, J. E., Gressani, V., Longepe, N., Vandemark, D., Foster, R. C., and Chapron, B.: Classification of the global Sentinel-1 SAR vignettes for ocean surface process studies, Remote Sens. Environ., 234, 111457, 2019b.